

Simultaneous measurement of thermo-optic and thermal expansion coefficients with a single arm double interferometer

JOSE FRANCISCO MIRAS DOMENEGUETI,¹ ACACIO A. ANDRADE,² VIVIANE PILLA,² AND SERGIO CARLOS ZILIO^{1,2,*}

¹Instituto de Física de São Carlos, Universidade de São Paulo, CP 369, 13560-970 São Carlos, SP, Brazil

²Universidade Federal de Uberlândia, Av. João Naves de Ávila 2121, 38400-902 Uberlândia, MG, Brazil

*zilio@ifsc.usp.br

Abstract: A low-cost single arm double interferometer was developed for the concurrent measurement of linear thermal expansion (α) and thermo-optic (dn/dT) coefficients of transparent samples with plane and parallel surfaces. Owing to its common-path optical arrangement, the device is compact and stable, and allows the simultaneous measurement of interferences arising from a low-finesse Fabry-Perot etalon and from a Mach-Zehnder-type interferometer. The method was demonstrated with measurements of solid (silica, BK7, SF6) and liquid (water, ethanol and acetone) samples.

© 2017 Optical Society of America

OCIS codes: (120.3180) Interferometry; (120.4530) Optical constants; (230.0230) Optical devices.

References and links

1. A. J. Werner, "Methods in high precision refractometry of optical glasses," *Appl. Opt.* **7**(5), 837–843 (1968).
2. J. M. Jewell, C. Askins, and I. D. Aggarwal, "Interferometric method for concurrent measurement of thermo-optic and thermal expansion coefficients," *Appl. Opt.* **30**(25), 3656–3660 (1991).
3. Y. Sato and T. Taira, "Highly accurate interferometric evaluation of thermal expansion and dn/dT of optical materials," *Opt. Mater. Express* **4**(5), 876–888 (2014).
4. W. V. Sorin and D. F. Gray, "Simultaneous thickness and group index measurement using optical low-coherence reflectometry," *IEEE Photonics Technol. Lett.* **4**(1), 105–107 (1992).
5. J. Na, H. Y. Choi, E. S. Choi, C. Lee, and B. H. Lee, "Self-referenced spectral interferometry for simultaneous measurements of thickness and refractive index," *Appl. Opt.* **48**(13), 2461–2467 (2009).
6. P. Hlubina, "White-light spectral interferometry with the uncompensated Michelson interferometer and the group refractive index dispersion in fused silica," *Opt. Commun.* **193**(1–6), 1–7 (2001).
7. A. C. P. Rocha, J. R. Silva, S. M. Lima, L. A. O. Nunes, and L. H. C. Andrade, "Measurements of refractive indices and thermo-optical coefficients using a white-light Michelson interferometer," *Appl. Opt.* **55**(24), 6639–6643 (2016).
8. G. D. Gillen and S. Guha, "Use of Michelson and Fabry-Perot interferometry for independent determination of the refractive index and physical thickness of wafers," *Appl. Opt.* **44**(3), 344–347 (2005).
9. J. A. Corsetti, W. E. Green, J. D. Ellis, G. R. Schmidt, and D. T. Moore, "Simultaneous interferometric measurement of linear coefficient of thermal expansion and temperature-dependent refractive index coefficient of optical materials," *Appl. Opt.* **55**(29), 8145–8152 (2016).
10. P. H. Tomlins, P. Woolliams, C. Hart, A. Beaumont, and M. Tedaldi, "Optical coherence refractometry," *Opt. Lett.* **33**(19), 2272–2274 (2008).
11. S. Kim, J. Na, M. J. Kim, and B. H. Lee, "Simultaneous measurement of refractive index and thickness by combining low-coherence interferometry and confocal optics," *Opt. Express* **16**(8), 5516–5526 (2008).
12. S. C. Zilio, "Simultaneous thickness and group index measurement with a single arm low-coherence interferometer," *Opt. Express* **22**(22), 27392–27397 (2014).
13. Y. H. Kim, S. J. Park, S. W. Jeon, S. Ju, C. S. Park, W. T. Han, and B. H. Lee, "Thermo-optic coefficient measurement of liquids based on simultaneous temperature and refractive index sensing capability of a two-mode fiber interferometric probe," *Opt. Express* **20**(21), 23744–23754 (2012).
14. D. Solimini, "Loss measurement of organic materials at 6328 Å," *J. Appl. Phys.* **37**(8), 3314–3315 (1966).
15. Heraeus-Quarzglas, Quartz Glass for Optics Data and Properties, (2014). <https://www.heraeus.com>
16. Schott, Optical Glass Data Sheets (2014). <http://www.schott.com>

1. Introduction

The accurate determination of thermal properties of optical materials is important in the development of new laser media, window materials and nonlinear optical devices. This knowledge is also of importance for the construction of accurate satellite cameras, where part of the equipment is subjected to sunlight and part to the cosmic background radiation, causing severe temperature gradients. For these applications, parameters like the index of refraction (n), thermo-optic coefficient (TOC, dn/dT) and the coefficient of linear thermal expansion (CTE, α) have to be precisely determined.

There are several techniques to measure these quantities and they can be roughly divided in two categories: those using the Snell-Descartes law and others based on interferometry, either with monochromatic or broadband light. Within the first category, there are refractometers based on the minimum deviation in a prism and on the critical and Brewster angles [1]. These techniques measure n with an accuracy ranging from 10^{-4} to 10^{-6} and can provide dn/dT , if the refractometer has the capability of changing the sample temperature, but not α . The other class of techniques, refractometry based on interferometry, provides more accurate means of obtaining the refractive index of different materials. For instance, a Fabry-Perot-type interferometer can be used for the concurrent measurement of α and dn/dT with good accuracy and reproducibility [2]. However, the mirrors have to be inside a tube furnace and the temperature cycling may degrade their performance with time. Furthermore, the beams are expanded, which may require samples with large areas, and a hole has to be drilled through the sample to allow the measurement of α . Another example of dn/dT measurements studying fringe shifts in the transmission of a light beam through a Fabry-Perot interferometer (FPI) under uniform heating is presented in [3] but there, a dilatometer is used to yield the value of α . This is necessary because the technique based on the FPI measures the optical path difference, which is proportional to the product of n and the thickness, in contrast to the setup in [2] that employed two FPI in parallel, one with the sample and the other with air.

The Michelson-type interferometer has also been used quite often to determine the refractive index of transparent samples. Here we restrict the discussion to setups that employ low-coherence light sources, named spectral-domain interferometry [4–7]. These devices are of two kinds: those that scan one of the interferometers mirrors to provide the index dispersion and others that Fourier transform the spectrum to yield the group index and thickness. If a heater is introduced to change the sample temperature, the thermo-optic coefficient can be determined for different wavelengths [7].

Techniques using a combination of Michelson and Fabry-Perot interferometers [8,9], modified optical coherence tomography (OCT) [10] and low-coherence interferometry with confocal optics [11] were also introduced, among others. We recently introduced a one-arm low-coherence interferometer that allows the measurement of the geometrical thickness and group index of plane-parallel optically transparent samples [12]. We hoped this device would be able to measure α and dn/dT because of the reduced noise and the available space for introducing an oven. However, the instrument did not present the necessary accuracy mainly because the portable spectrometer does not have the required resolution. The present work reports on a low-cost monochromatic single arm double interferometer that presents both Fabry-Perot and two-beam interferences. This device is able to measure solid and liquid samples, with a typical accuracy of $0.5 \times 10^{-6} \text{ } ^\circ\text{C}^{-1}$ for both α and dn/dT in solids and $2 \times 10^{-5} \text{ } ^\circ\text{C}^{-1}$ for dn/dT in liquids.

2. Experimental section

The experimental setup, schematically shown in Fig. 1, is similar to that employed in [12]. It uses a low-cost 532 nm laser pointer that impinges on a beam-splitter (BS1) made of float glass from an ordinary soda lime house window. Owing to its fabrication process, such a window has plane surfaces fairly parallel and generates a pair of beams with nearly the same

intensity. Additional beams (dashed lines) are blocked by beam stoppers. A bandpass Schott BG39 filter (not shown in the figure) was added to block the 808 nm light from the diode laser that pumps the Nd:YVO₄ crystal. Beam 1 (external reflection in BS1) passes through the sample, impinges on BS2 and its internal reflection is directed to a detector (MZD). The external reflection of beam 2 on BS2 is also directed to the same detector and interferes with beam 1 with a phase mismatch of $\phi^{MZ} = (2\pi/\lambda)(n-1)t$, where n is the index of refraction of the sample, t is its thickness and $\lambda = 532$ nm. We used a superscript MZ because this two beam interferometer resembles a Mach–Zehnder interferometer and for this reason the detector was named MZD. Part of beam 2 is transmitted through BS2 and impinges on a normalizing detector (ND) whose signal is used to correct any intensity fluctuation in the experiment. On the other hand, beam 1 reflects on both surfaces of the sample, giving rise to interference pattern typical of a low finesse Fabry-Perot etalon, with a phase mismatch of $\phi^{FP} = (4\pi/\lambda)nt$, and then goes to another detector (FPD). As the temperature changes, both n and t change, as a consequence of the thermal expansion and the thermo-optic effect, respectively. Therefore, by using a thermo-electric heater (TEH) based on the Peltier effect to change the temperature of the sample, one obtains fringe patterns as those shown in Fig. 2. These patterns are acquired by a National Instruments data-acquisition (DAQ) module and analyzed with a personal computer with the LabVIEW software. The temperature of the Peltier device is also controlled by the DAQ and computer.

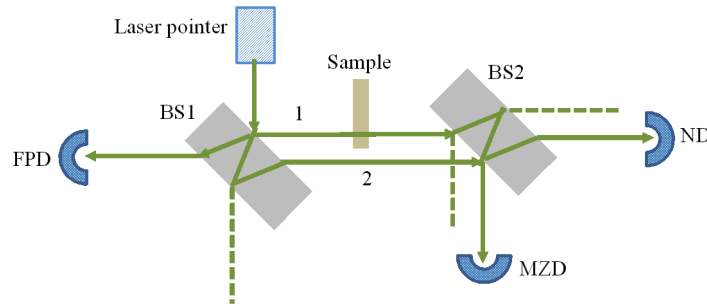


Fig. 1. Schematic view of the single-arm double interferometer: BS1 and BS2 are beam splitters, and FPD, MZD and ND are silicon photo-detectors.

Substituting the temperature variations of n and t , given as $n = n_0 + \frac{dn}{dT}\Delta T$ and $t = t_0(1 + \alpha\Delta T)$, in the expressions of ϕ^{FP} and ϕ^{MZ} , we obtain the spacing between consecutive maxima and minima generated by each detector according to the equations:

$$\frac{dn}{dT} + n\alpha = \frac{\lambda}{4t_0\Delta T^{FP}} \quad (1)$$

for the Fabry-Perot etalon and

$$\frac{dn}{dT} + (n-1)\alpha = \frac{\lambda}{2t_0\Delta T^{MZ}} \quad (2)$$

for the Mach–Zehnder interferometer, where ΔT^{FP} and ΔT^{MZ} are the temperature spacing between consecutive maxima and minima of the Fabry-Perot and the Mach–Zehnder interferometers, respectively. From results like those of Fig. 2, the software finds the maxima and minima of each pattern, resulting in curves like those of Fig. 3, which provide the values of ΔT^{FP} and ΔT^{MZ} for each index that corresponds to a given temperature. These values are fed into Eqs. (1) and (2) yielding α and dn/dT as:

$$\alpha = \frac{\lambda}{2t_0} \left[\frac{1}{2\Delta T^{FP}} - \frac{1}{\Delta T^{MZ}} \right] \quad (3)$$

and

$$\frac{dn}{dT} = \frac{\lambda}{2t_0} \left[\frac{n}{\Delta T^{MZ}} - \frac{(n-1)}{2\Delta T^{FP}} \right] \quad (4)$$

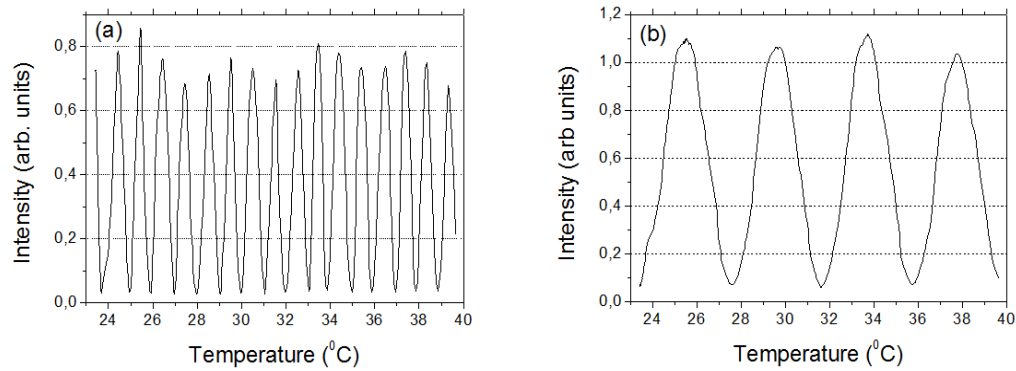


Fig. 2. Fringe patterns for the Fabry-Pérot (a) and Mach-Zehnder (b) interferometers in a 20 mm-thick sample of BK7 glass.

For solid samples, these values are usually constants in the temperature range studied (< 40 °C), but for liquid solutions they may change, as we see for the case of water. For liquids, we do not measure the thermal expansion because it just increases the height inside the cuvette. By neglecting the cuvette glass expansion, it is enough to use Eq. (2) with $\alpha = 0$ to obtain the value of the TOC.

Figures 2 and 3 refer to a Schott BK7 glass sample that was glued with a heatsink plaster to the TEH together with the thermocouple. For liquid samples, the 1-mm optical path cuvette containing the solution is placed inside the U-shaped copper holder shown in the inset of Fig. 4 such that natural convection is minimized. The sample thickness is an important parameter to be considered - if the sample is optically too thin fewer fringes will be observed per temperature interval and the sample has to be heated more. This may cause thermal misalignment of the system and evaporate liquid solutions as acetone for instance. On the other hand, if the sample is optically too thick, too many fringes are observed and the thermocouple does not have enough accuracy to yield good results. For a suitable thickness we have $\Delta T^{FP} \sim 1$ °C and $\Delta T^{MZ} \sim 5$ °C. Furthermore, the heating rate is set below 0.5 °C/min to guarantee the temperature uniformity.

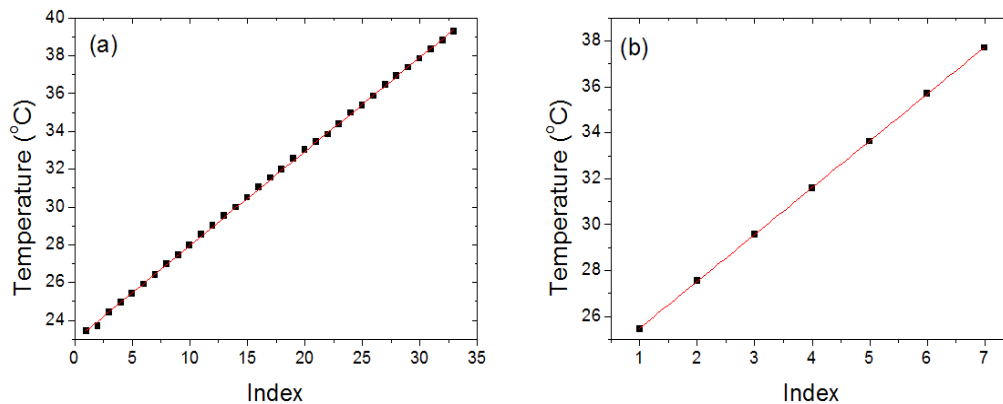


Fig. 3. Temperature of consecutive maxima and minima for patterns observed in Fig. 2 for the Fabry-Pérot (a) and Mach-Zehnder (b) interferometers. The index origin was arbitrarily chosen.

3. Results and discussion

In order to validate the method, measurements were carried out on liquids (water, ethanol and acetone) and transparent solids (silica, BK7 and SF6). The black solid squares in Fig. 4 show results obtained for distilled water placed in a 1-mm thick cuvette in the range 30–65 °C while the red dots are results obtained with a high accuracy commercial refractometer (Atago RX5000- α). The error bars are related to the uncertainty in obtaining ΔT 's used in Eq. (1), as discussed in Section 4. A very good agreement is observed between the two measurements.

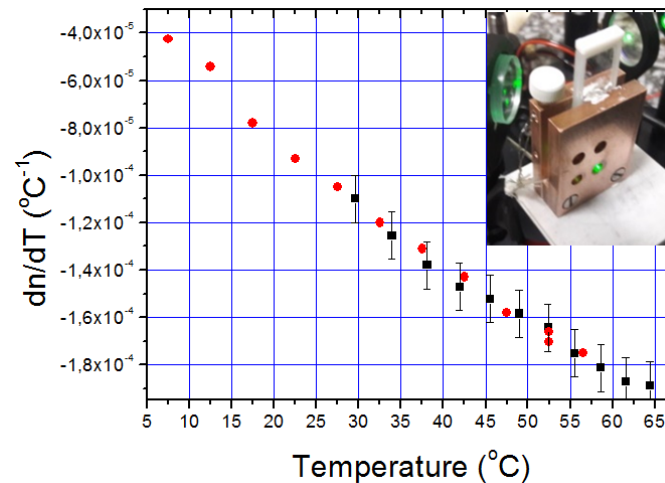


Fig. 4. Thermo-optic coefficients of water obtained with the present setup (black squares) and a commercial refractometer (red circles). The inset shows the cuvette holder.

The results for ethanol and acetone are depicted in Fig. 5 and the averaged TOCs are listed in Table 1. Since ethanol and acetone are quite volatile, the temperature range and the measurement time were reduced to avoid significant evaporation. Accordingly, the fluctuations of the experimental points are higher than those of water.

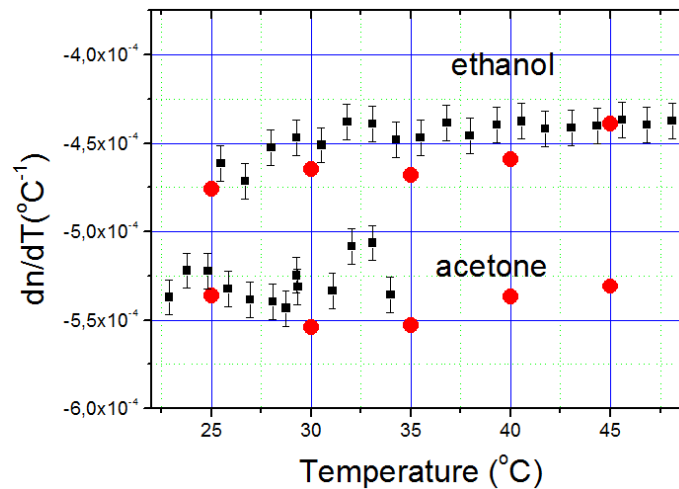


Fig. 5. Thermo-optic coefficients of ethanol and acetone obtained with the present setup (black squares) and a commercial refractometer (red circles).

Ethanol and acetone samples were already studied at 1550 nm [13] and 632.8 nm [14]. The reference values in Table 1 were obtained from [14] and are somewhat different from our values probably because we measured at 532 nm. However our results are in good agreement with those obtained with the commercial refractometer.

Table 1. Averaged thermo-optic coefficients for ethanol and acetone

| Sample | dn/dT ($10^{-4} \text{ } ^\circ\text{C}^{-1}$) | | |
|---------|----------------------------------------------------|---------------|-----------|
| | Meas. (532 nm) | Ref. (633 nm) | Diff. (%) |
| Ethanol | -4.4 | -4.0 | 10 |
| Acetone | -5.3 | -5.0 | 6 |

The solid samples measured were Heraasil quartz (trade name of a particular type of silica made by Heraeus-Quarzglas) and two types of Schott optical glasses: a crown (BK7) and a flint (SF6) glass. The relevant data to be used as reference can be found in [15] and [16]. The thicknesses were measured with a caliper rule. All experimental results obtained are similar to those presented in Fig. 2, which can be used to provide the points of Fig. 3. If these points can be fitted with a straight line, α and dn/dT are constants. Otherwise, the departure from the straight line indicates that these parameters change with the temperature. In this case, the ΔT 's have to be found for each inter-fringe to provide the temperature dispersion of α and dn/dT .

Table 2. Thermo-optic and thermal expansion coefficients for solid samples

| Sample | Thickness (mm) | dn/dT ($10^{-6} \text{ } ^\circ\text{C}^{-1}$) | | | α ($10^{-6} \text{ } ^\circ\text{C}^{-1}$) | | |
|--------|----------------|----------------------------------------------------|------|-----------|-----------------------------------------------------|------|-----------|
| | | Meas. | Ref. | Diff. (%) | Meas. | Ref. | Diff. (%) |
| Silica | 4.90 | 10.16 | 10.2 | 0.4 | -0.12 | 0.55 | ~120 |
| BK7 | 20.15 | 2.94 | 3.0 | 1.9 | 6.80 | 7.10 | 4.1 |
| SF6 | 3.50 | 11.4 | 11.1 | 2.3 | 8.02 | 8.10 | 1.0 |

Concerning to the accuracy of the technique, the main source of error is the inaccuracy in the measurement of ΔT . For liquid samples, dn/dT is given by: $dn/dT = \lambda / (2t_0 \Delta T^{M/Z})$, implying in an accuracy of $\approx 2 \times 10^{-5} \text{ } ^\circ\text{C}^{-1}$ for the 1 mm-thick cuvette, $\lambda = 0.532 \text{ } \mu\text{m}$ and an uncertainty of $\pm 0.05 \text{ } ^\circ\text{C}$ in $\Delta T^{M/Z} \approx 1 \text{ } ^\circ\text{C}$. This justifies the error bars in Figs. 4 and 5. For solid samples, the thickness is larger by a factor of about 10, ΔT 's are on the order of $5 \text{ } ^\circ\text{C}$, and according to Eqs. (4) and (5), the accuracy is $\approx 0.5 \times 10^{-6} \text{ } ^\circ\text{C}^{-1}$. This is in agreement with the values found in Table 2. Another source of error occurs when either α or dn/dT are too small, as happens for the

thermal expansion of silica. In this case, $\Delta T^{MZ} \approx 2\Delta T^{FP}$ as predicted by Eqs. (1) and (2), the two terms in brackets in Eq. (3) are nearly equal and their difference introduces significant errors in the results. To improve the accuracy of the present technique, more accurate means of measuring the temperature have to be employed. Anyway, this is a technical problem, not a fundamental limitation.

5. Conclusions

In summary, we proposed a device composed of a one-arm double interferometer that allows the simultaneous measurement of thermo-optic and thermal expansion coefficients of plane-parallel optically transparent samples. The two beams generated at the first beam-splitter propagate through a nearly common path and this makes the device very compact and stable, nearly immune to mechanical vibrations. Another advantage of sharing the same optical path is that any air drift is automatically compensated. Furthermore, the optical device has no moving parts, needs just one measurement to provide Fabry-Perot and Mach-Zehnder fringes, and the sample can be placed in any position along the optical path. The accuracy is typically around 0.5 ppm, but can be improved if a better thermometer is used.

Funding

Fundação de Amparo à Pesquisa do Estado de Minas Gerais (APQ-02062-14); Conselho Nacional de Desenvolvimento Científico e Tecnológico (573916/2008-0). Coordenação de Aperfeiçoamento de Pessoal de Nível Superior (fellowship for SCZ).